Electronic Supplementary Material (ESI) for Journal of Materials Chemistry A.

Supporting information: Biomimetic wiring and stabilization of photosynthetic membrane proteins with block copolymer interfaces

Patrick O. Saboe,[a] Emelia Conte,[a] Stanley Chan,[a] Hasin Feroz,[a] Bryan Ferlez,[b] Megan Farell, [a] Matthew F. Poyton,[c] Ian T. Sines,[a] Hengjing Yan,[d] Guillermo C. Bazan,[d] John Golbeck,[e] and Manish Kumar, [a,*]

a. Department of Chemical Engineering, The Pennsylvania State University, University Park, PA 16802, USA
b. Department of Biochemistry and Molecular Biology, The Pennsylvania State University, University Park, PA 16802, USA
c. Department of Chemistry, The Pennsylvania State University, University Park, PA 16802, USA
d. Center for Polymers and Organic Solids, University of California at Santa Barbara, Santa Barbara, CA 93106, USA
e. Department of Chemistry, and Department of Biochemistry and Molecular Biology, The Pennsylvania State University, University Park, PA 16802
** Corresponding authors*

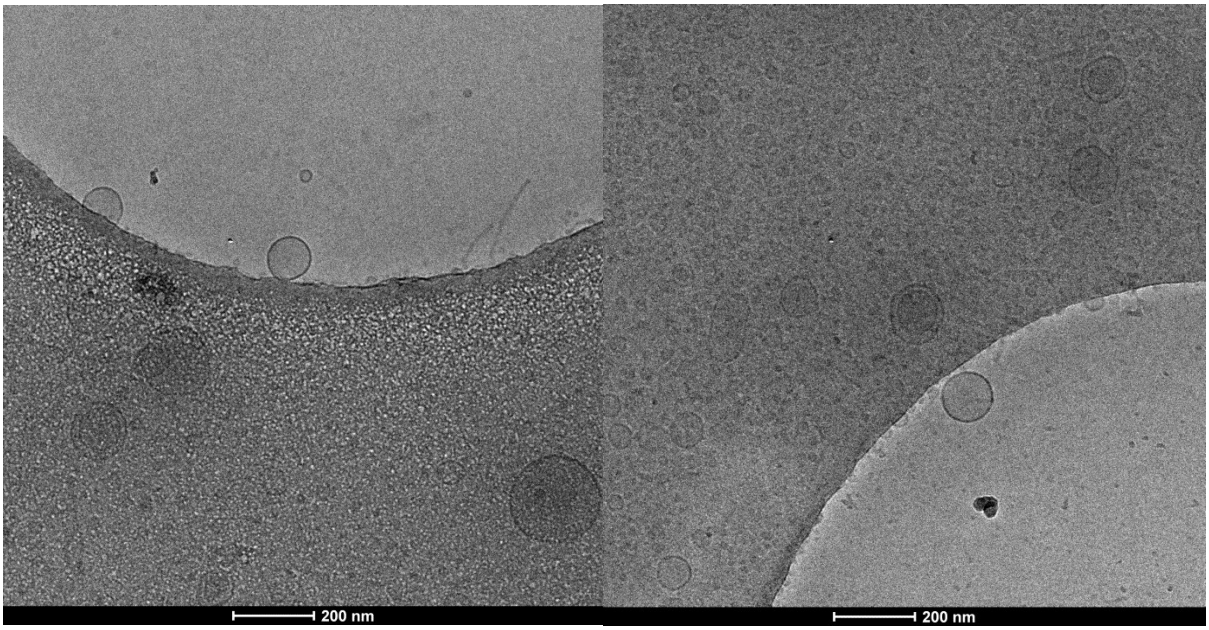

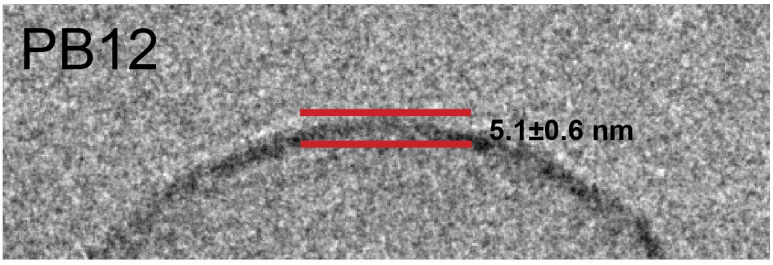

Figure S1. (Top) Cryo-TEM of small unilamellar vesicles (SUVs) formed from poly(butadiene)$_{12}$-poly(ethylene oxide)$_8$ (PB_{12}-PEO_8). Vesicles were self-assembled by using film rehydration, extrusion, and were approximately 100-200 nm in diameter after processing. **(Bottom)** The average hydrophobic block thickness of the PB-PEO vesicles was 5.1 ± 0.6 nm as determined from cryo-TEM imaging.

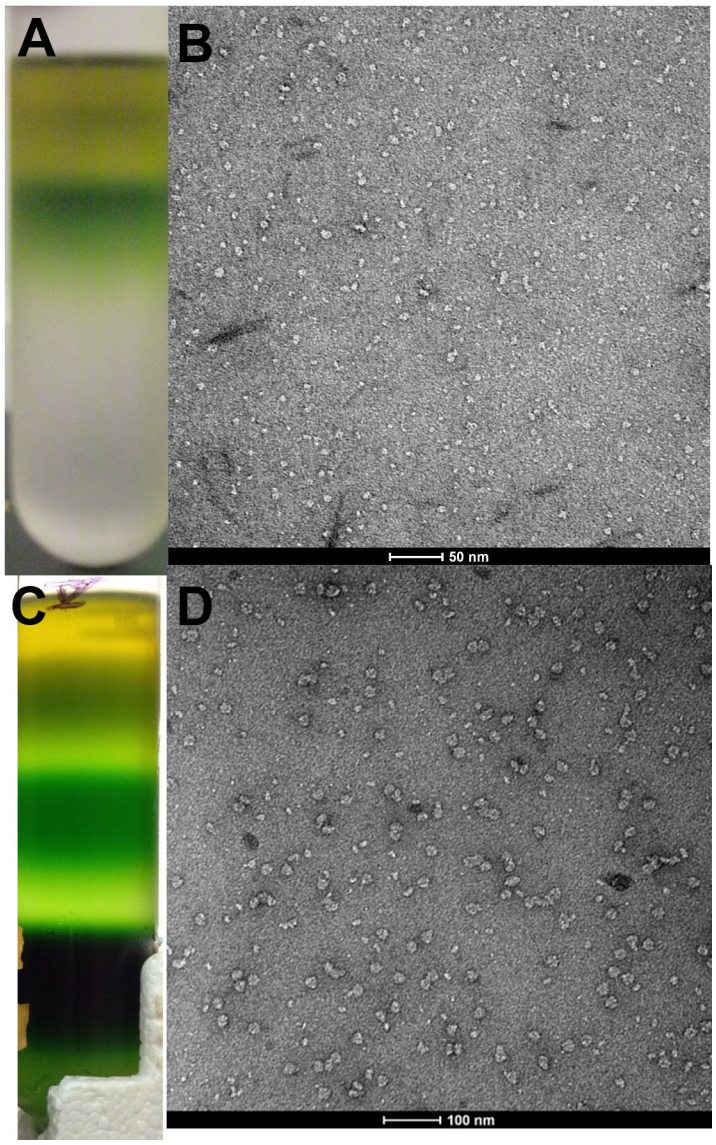

Figure S2: The PSI protein was isolated from cyanobacteria using sucrose gradients. A) PsaL deficient *PsaJ*-his_6-tagged PSI was isolated from *Synechococcus sp.* PCC 7002 using a sucrose gradient. Monomeric PSI runs as the lowest green band on a sucrose gradient after thylakoid solubilization B) After size exclusion, the monomeric protein was imaged using negative stain. C) Native PSI was from *Synechococcus sp.* PCC 7002 was similarity purified using sucrose gradients. The lowest dark band was collected and imaged by negative stain TEM (D).

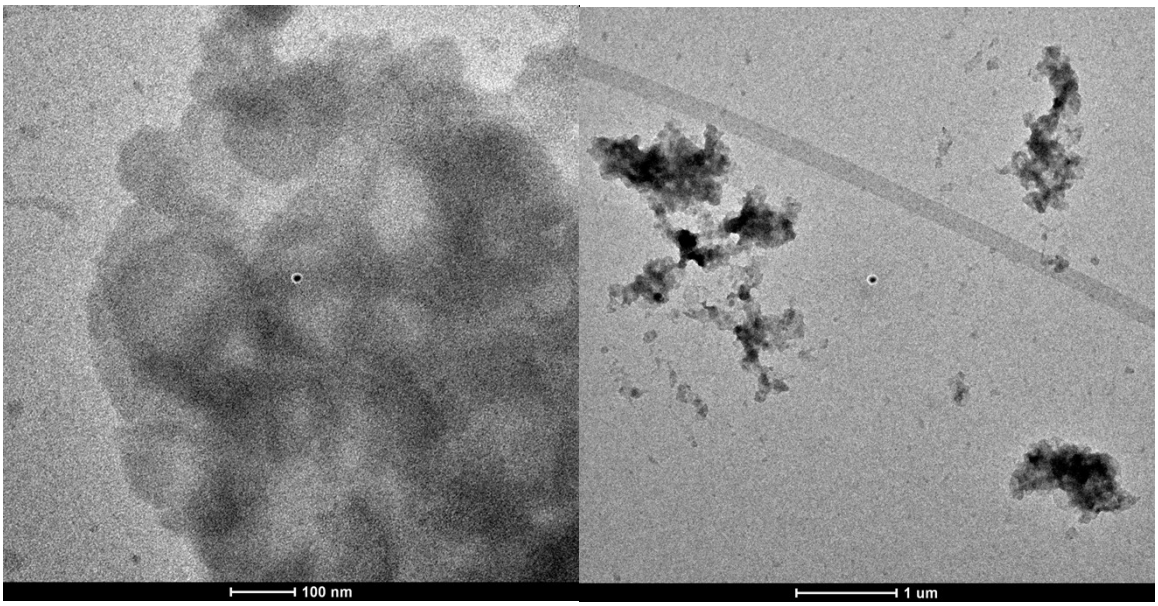

Figure S3: We used both monomeric (Figure S2-B) and trimeric PSI (Figure S2-D) for BCP reconstitution. We observed that both monomeric (Figure 3A) and trimeric protein (Figure S3) incorporate into BCP membranes at PoPR 0.5-1.0. The PSI membranes aggregate into 1 μm or larger clusters as shown by the negative stain image on the right. We did not observe crystallinity of either monomer or trimeric PSI protein in block copolymer membranes (see results and discussion for further explanation). We choose to use trimeric PSI protein for all spectroscopy and photocurrent measurements since monomeric PSI purifications required extended processing time in high detergent conditions, which may lead to decoupled chlorophyll (See Figure S14). Furthermore, we did not find it necessary to use a Ni-NTA immobilization strategy to generate significant photocurrents.

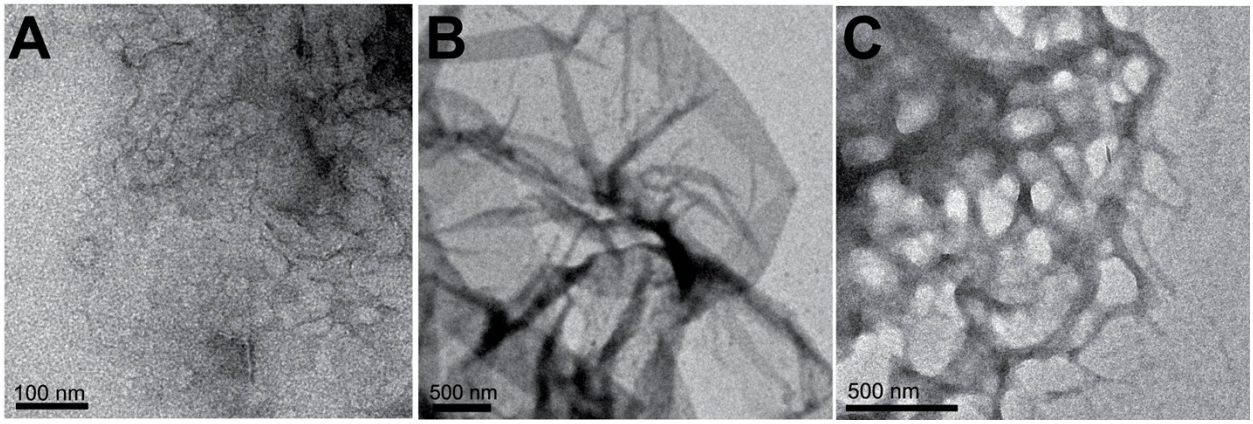

Figure S4: Protein reconstituted within block copolymers (BCPs) at different w/w polymer-protein (PoPR) ratios influence the overall morphology of the membrane. Low PoPRs represent a higher concentration of proteins in membranes. A) At PoPRs below 0.5, only small, disordered PSI-BCP aggregates were formed. Similar disordered protein aggregates are formed when there are very low amount of lipids in a 2D crystallization sample (low lipid-to-protein ratio or LPR)[1]. At a PoPR between 0.5 and 1, photosystem I (PSI) forms large, two-dimensional (2D) sheets with PB_{12}-PEO8. These membranes exhibit unilamellarity with a high packing of PSI within the membrane. C) PoPRs greater than 2 cause folding of the membrane sheets into three-dimensional (3D) membrane networks due to the lower membrane concentration of PSI. Large membranes as shown in Fig S4b are ideal for bioelectric devices, as PSI is densely packed into the membrane and oriented within the membrane to enable photosynthetic electron transfer across the membrane similar to that seen in biological photosynthetic membranes. Since large membranes were only observed at PoPR 0.5 to 1.0, these samples were exclusively used for photocurrent measurements.

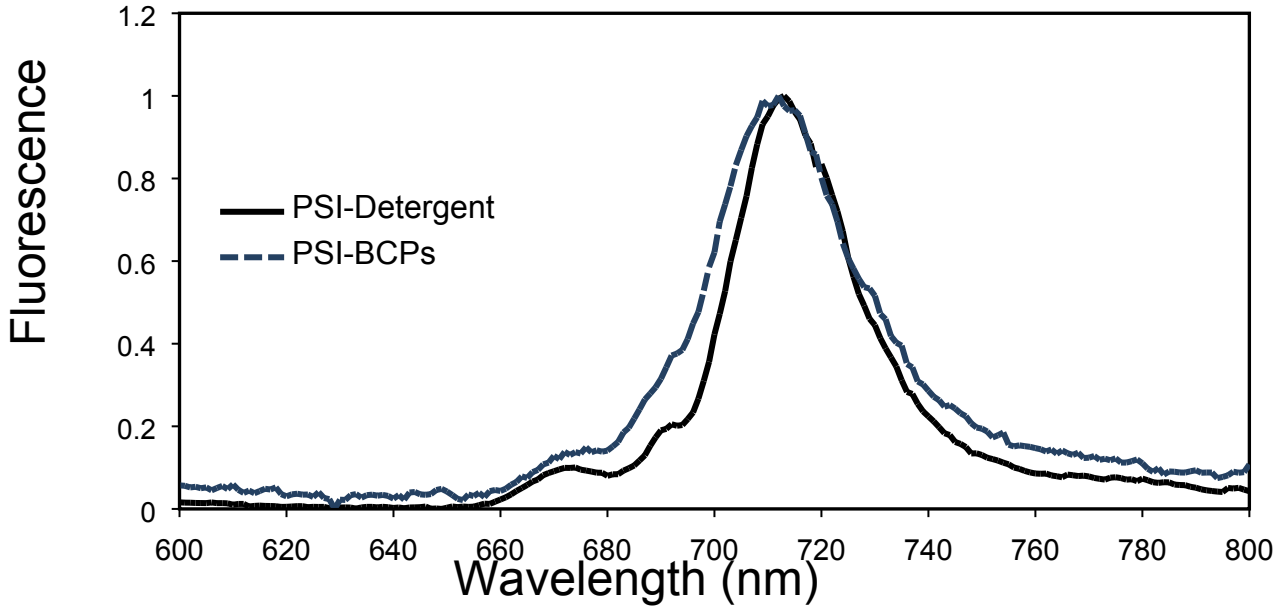

Figure S5. The 77K fluorescence signal of both PSI in detergent micelles and in BCP membranes was measured and show a single peak at 715 nm.[2] The overlapping of signals indicated that BCPs did not influence the structure/binding of the chlorophyll cofactors of PSI.

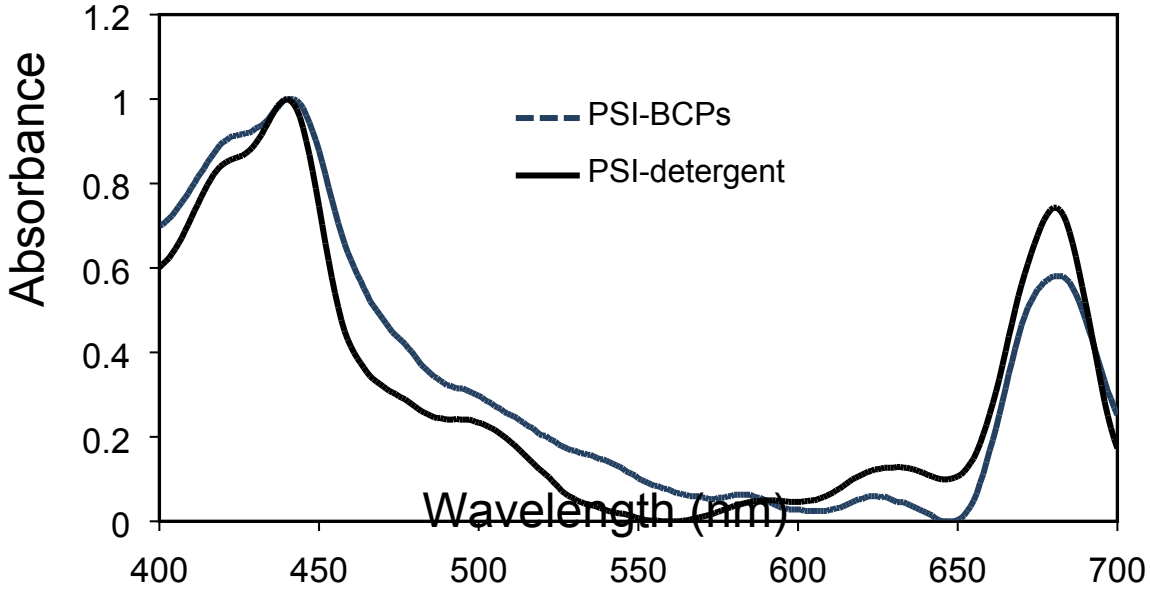

Figure S6. The UV-Vis spectra of both PSI in detergent micelles and in BCP membranes were generated. The overlapping spectra show that the BCPs did not influence the overall absorbance properties of the protein.

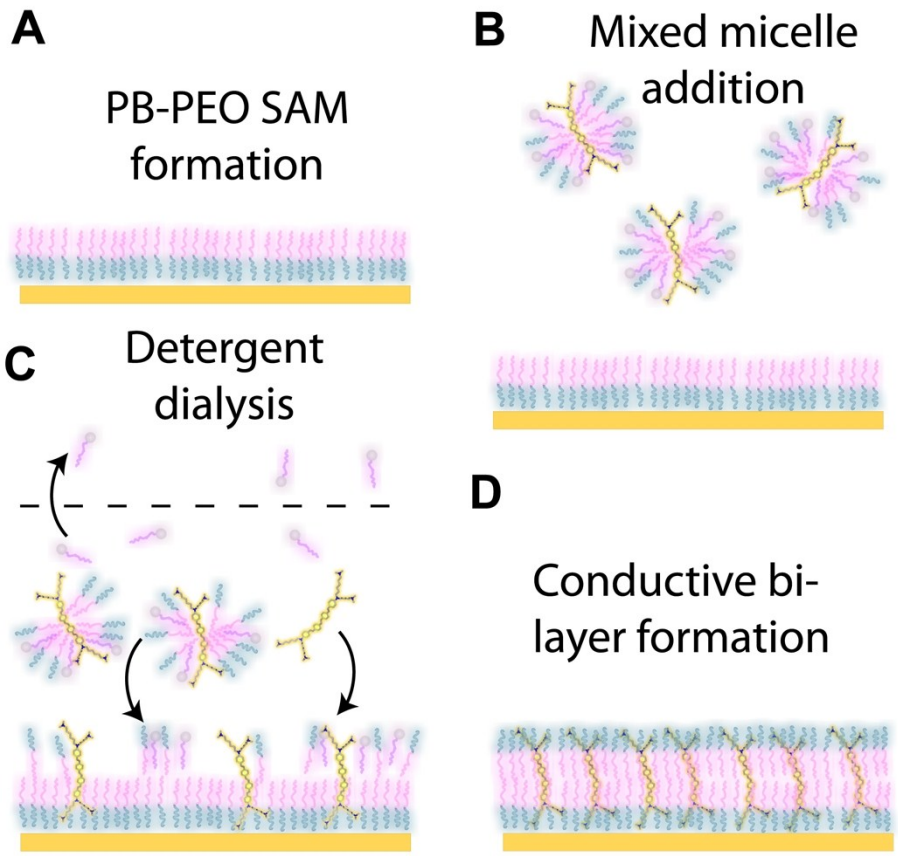

Figure S7. A) A self-assembled monolayer (SAM) of thiolated PB-PEO polymer was formed on a gold coated slide (in chloroform). **B)** An initial concentration of 0.05 mg/mL PB-PEO, 25 mol % DSSN+ with respect to the polymer, and 5%OG was added to the electrode after SAM formation. PB-PEO, DSSN+ and OG form micelles **C-D)** A dialysis membrane (10-12 kDa cutoff) was added above the electrode to remove the OG. Detergent was removed by dialysis using a buffer of 100mM NaCl, 50 mM Tris pH 8.3, and 3 mM NaN3. As the OG is removed, a thin-film of PB-PEO and DSSN+ is formed on the electrode surface. A photo of a typical dialysis-electrode cell is provided below **(Figure S6).**

Figure S8. A typical dialysis-electrode set-up. A gold electrode is clamped (aluminum clamp) to a glass O-ring-joint. A dialysis membrane is then fit onto the opening of the glass cell using a modified dialysis button (Hampton Research, Aliso Viejo, CA). The cell volume is approximately 3 mL. To remove the detergent, the cell was placed in a large volume (1 L) of dialysis buffer (100mM NaCl, 50 mM Tris pH 8.3, and 3 mM NaN_3) for 3 days. The dialysis buffer was replaced every 24 hours. After 3 days the dialysis button was removed and the electrochemical buffer was added.

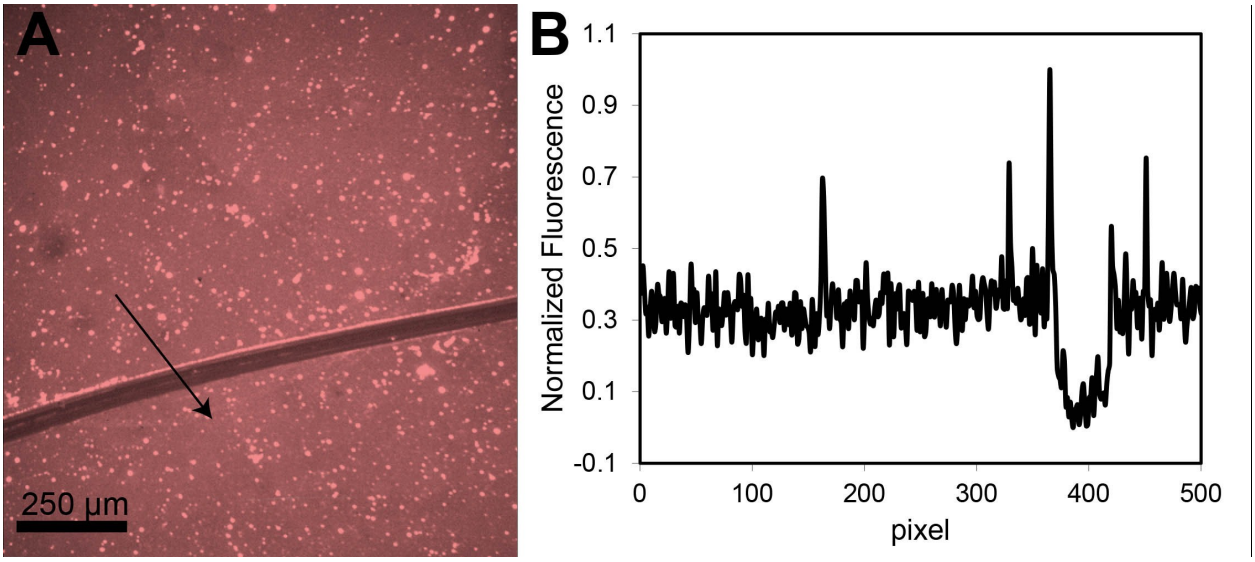

Figure S9. Fluorescent signal from bilayer electrodes with DSSN+. The surface was functionalized as described in **Figure S5-S6**. **A)** The fluorescent signal of the DSSN+ (2 mol% relative to the PB-PEO) is observable above background (the dark band is a region of the film that has been removed by scratching the electrode with tweezers). The fluorescent signal shows good spreading and absorption of the polymers onto the gold surface. **B)** The line-scan of fluorescence intensity along the black in Figure S7A. Here, the background is subtracted and the normalized data was plotted. The minimum fluorescence intensity in the scratched region was taken to be the background intensity.

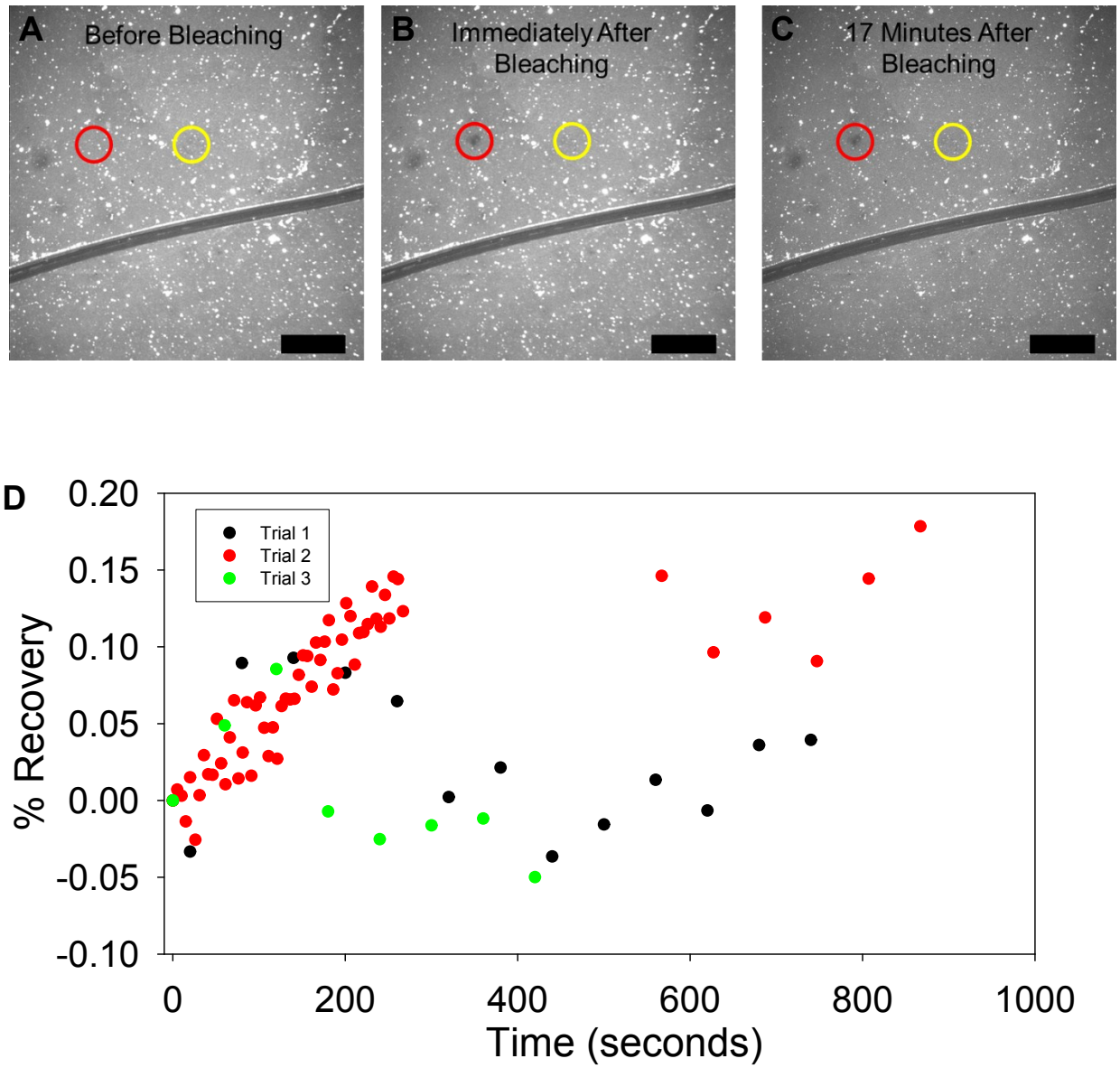

Figure S10. Fluorescence recovery after photobleaching (FRAP) **A)** The polymer coated electrode before DSSN+ bleaching, **B)** immediately after DSSN+ bleaching and **C)** 17 minutes after bleaching. The scale bar in each image is 240 micrometers in length. The red circle indicates the bleached region and the yellow region is the control region used to normalize the fluorescence as described in the methods section. The dark region that spans the image from left to right is a scratch where some of the polymer has been removed with tweezers. **D)** The FRAP

recovery curves for three separate FRAP experiments on two different polymer coated electrodes. Lipid lateral diffusion within tethered lipid bilayers is known to be disrupted due to tethering, especially at high concentrations of tethering lipid.[3] We used a high molar percentage of tethering block copolymer (17 mol %) within the self-assembled monolayer. Note that block copolymers[4] and the oligomer DSSN+[5] have a later diffusion coefficient that is two orders of magnitude less than lipids.[3]

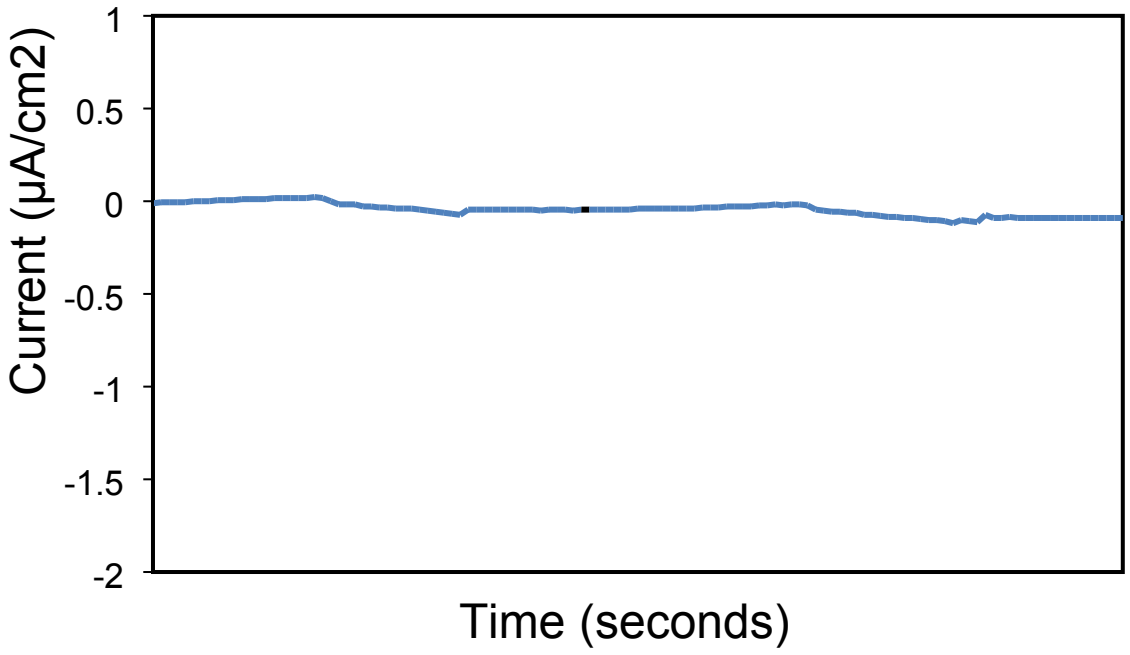

Figure S11. Zero photocurrent is produced from PB-PEO membranes without DSSN+ molecules. Light was provided to the electrode during the intervals of 10-20 seconds and 40-50 seconds. An immeasurable amount of photocurrent was detected.

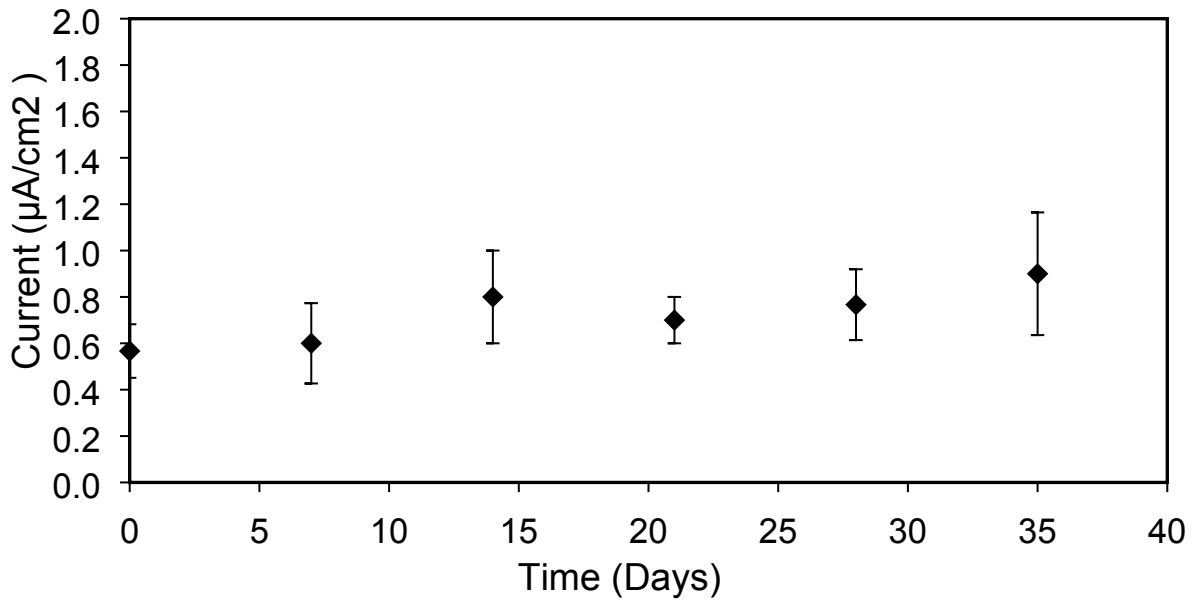

Figure S12. Stability testing of the DSSN+/COE bilayer was conducted weekly over a 35 day time span. Average photocurrent produced is represented, and typically ranges between 0.6 and 0.8 µA/cm^2.

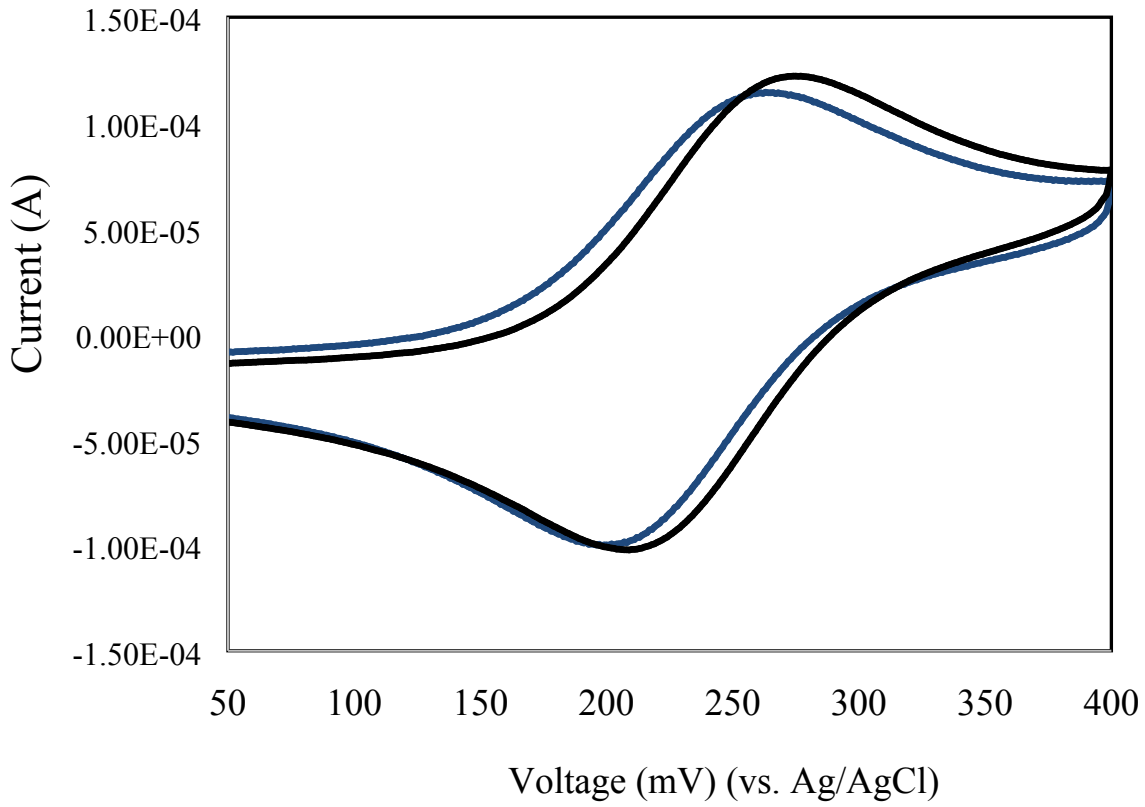

Figure S13. BCP-COE interface before (solid line) and after (dotted line) UV polymerization reaction. UV exposure is known to cross link side chains of polybutadiene (PB). We show that cross-linking PB does not influence the conductivity of the interface and is an excellent, robust material for long-term utilization.

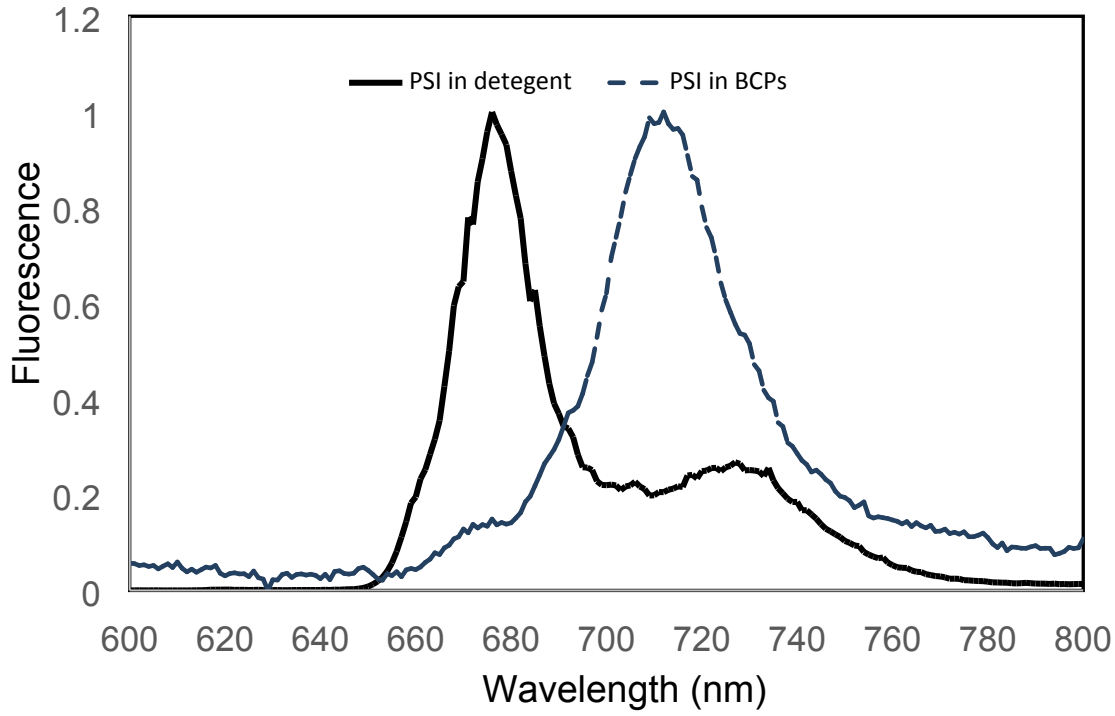

Figure S14: PSI was stored in dark conditions with 0.5% OTG for 30 days at 4 ºC. After 1 month, a 77K spectrum was taken to assay the stability of the PSI (solid black line). We observed that a peak at 675 nm, corresponding with detached chlorophyll in detergent micelles. PSI block copolymer membranes were stored in similar conditions (without OTG). We observed at single peak at 715 nm, indicating that PB-PEO BCP membranes did not disturb chlorophyll within PSI. Unlike detergent micelles, BCP membranes provide a compatible hydrophobic environment for long-term stabilization of PSI that mimics the native lipids.

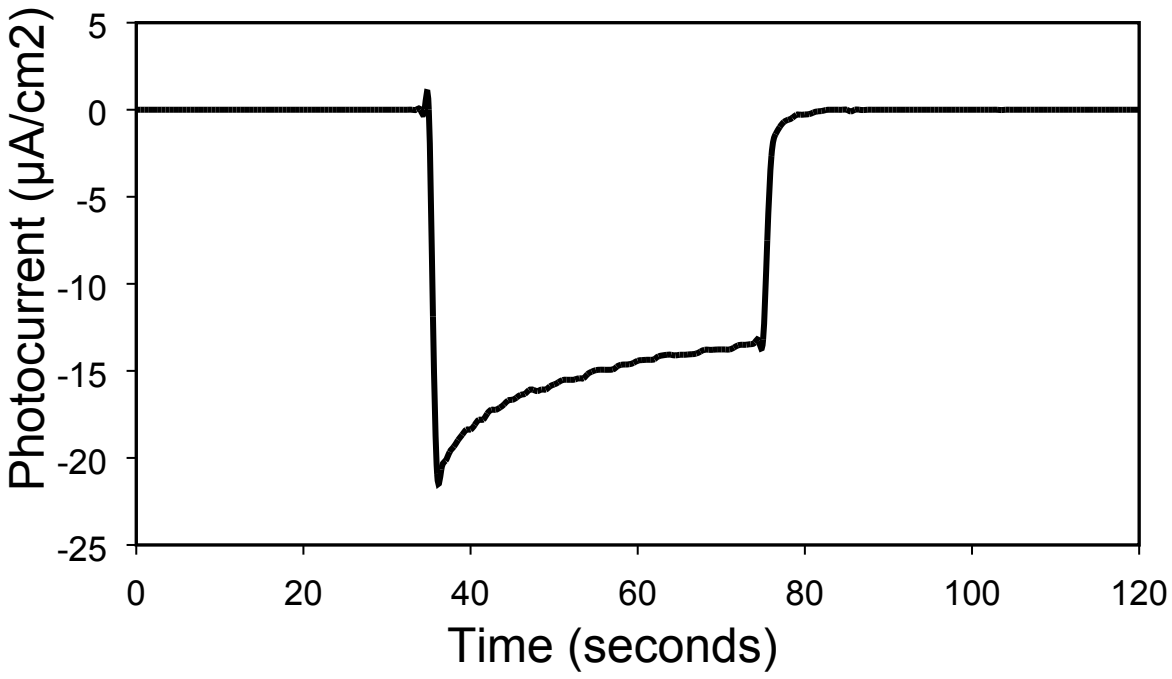

Figure S15. Four devices were tested for long term activity. The tested devices maintained a total activity of 100% to 60% of the original photocurrent when tested after 30 days. The decrease in photocurrent could be due to loose association of the PSI with the electrode surface. The PSI layer may have been disrupted during electrolyte buffer exchange. The PSI was electrostatically immobilized on the surface (covalent binding strategies were not implemented in this study).

Table S-1: Longevity and PSI matrix comparison of state-of-the-art PSI devices

Reference	Electrode interface	photocurrent ($\mu A/cm^2$)	photocurrent (µA/mg PSI)	Stability (days)	Activity Retention	light intensity mW/cm^2	Electron Mediator
This study	DSSN+/PB-PEO modified electrode, PB-PEO/PSI membranes	35	1250	30	~100%	20	100 µM PMS, 100 µM $K_3Fe(CN)_6^{-3}/K_4Fe(CN)_6^{-4}$, 2 mM MV
Terasaki *et al.* (2007)	1,4-benzenedimethanethiol SAM on gold with vitamin K_1 linked to Au-NP (~1.6 nm), 12-phenoxydodecyl)-triethylammonium bromide	~0.019	27	365	~100%	3.3	250 mM NaAsc, 2.5 mM DCIP
Manocchi *et al.* (2013)	Mercaptohexanol SAM with $Os(bpy)_2Cl_2$ mediator, 0.03% (n-dodecyl-β-D-maltoside) DDM detergent	0.035	228	>0.25	~100%	1.4	250 µM MV and 13.5 µM $Os(bpy)_2Cl_2$.
Ciesielski et al. (2010)	PSI multilayer on unmodified gold electrode, 0.05% Triton-X 100 surfactant	3	n/a	280	~75%	95	5 mM DCIP,100 mM NaAsc
Kothe *et al.* (2014)	poly(vinyl)imidazole Os-$(bipy)_2Cl$, 0.03% (w/v) n-dodecyl-b-D-maltoside (b-DM)	80	12600	0.625	0%[a]	1	poly(vinyl)imidazole Os-$(bipy)_2Cl$

a) Operated under continuous illumination

Longevity and PSI matrix comparison of state-of-the-art PSI devices

Table S-1 summarizes the current literature that has examined the photocurrent longevity of PSI devices. The work presented in this study has the highest photocurrent on a 30-day basis. Our photocurrent is an order of magnitude greater than all other studies that were studied for 30 days or longer. In addition, we built the only device that stabilizes PSI in a detergent-free environment. Although most of the studies that use detergent were stable for months, the photocurrent currents for these devices were relatively low and the activity retention of the devices were 75 to 100%. Kothe et al. (2014) generated high photocurrents were there device, however, a multiple day study was not tested.

Experimental

Block copolymer synthesis and functionalization: Poly-(butadiene)-poly(ethylene oxide) block copolymers were synthesized using anionic polymerization following a modified procedure by Bates and co-workers.[6] First, synthesis of 1,2-polybutadiene was conducted in tetrahydrofuran using sec-butyl lithium as initiator at -65 °C. Polymerization was terminated by addition of ethylene oxide yielding monohydroxyl-terminated polybutadiene. Polyethylene oxide growth was accomplished by converting the hydroxyl group to potassium alkoxide, which was used as a macroinitiator. Polyethylene oxide was functionalized with a carboxyl end group following Nehring *et al.*[7] Polyethylene oxide was functionalized with a thiol end group following Belegrinou *et al.*[8] Using NMR and GPC, we determined the degree of polymerization to be PB_{12}-PEO_8.

Giant unilamellar vesicle (GUV) assembly: GUVs were constructed based on the cross-linked dextran (ethylene glycol) hydrogel protocol by Kros and coworkers.[9] Glass slides were first cleaned in 1:1 volume ratio of HCl:methanol for one hour, rinsed with water, air-dried and left

overnight in a glove box to exclude atmospheric moisture.[10] Next, the slides were thiol-functionalized by soaking in 2% (by volume) 3-mercaptopropyl trimethoxysilane in toluene for 1 hour and rinsed thrice in toluene in a glove box. After the reaction was complete, the slides were taken out of the glove box, rinsed with water and stored before further use. The hydrogel was next prepared to coat the glass slides. Maleimide-dextran and thiol conjugated PEG purchased from Cellendes GmbH (Reutlingen, Germany) were mixed in a 1:1 molar ratio and 420 μL of 2mM of the mixture immediately pipetted onto the glass slide. This mixture was then covered with a piece of parafilm to ensure uniform layer formation on glass. A homogenous polymeric film was formed after 30–45 minutes at 40 °C. Next, 10 μL of 1 mg/ml BCP, PB_{12}-PEO_8 in chloroform was pipetted on to the hydrogel and dried for 30 minutes under vacuum at room temperature. Next, the BCP film was hydrated in a GUV well/growth chamber formed by placing a X-profiled O-Ring on top of the hydrogel and sealing with high vacuum silicon grease. Finally, the BCP film was hydrated with 300 μL of water and left at 40 °C for 1–2 hours to form free-floating vesicles.

Confocal microscopy and fluorescence excitation and emission measurements: Prior to imaging using a Leica TCS SP5 confocal microscope (LSCM, Leica Microsystems), 5 μM final concentration of DSSN+ was added to the GUVs. The emission and excitation of the DSSN in GUVs and in solution was measured using plate reader, Spectramax i3 (Molecular Devices, CA).

Growth and isolation of Photosystem I (PSI): PSI and PsaL deficient *PsaJ*-his_6-tagged PSI was isolated from *Synechococcus sp.* PCC 7002,[11] grown in A+ medium, supplemented with vitamin B12, 3% CO_2 (air balanced) bubbling, 100 μmol photons m^{-2} s^{-1}, at 37˚C. PSI trimers was isolated as described previously.[11, 12] Protein concentration was measured by the Bicinchoninic acid (BCA) assay.

Block copolymer Photosystem I membrane assembly: PSI and PsaL deficient *PsaJ*-his_6-tagged PSI was isolated from *Synechococcus sp.* PCC 7002[11] PSI particles were processed for reconstitution as described[12]. Briefly, the protein was size excluded and precipitated using PEG6000/$MgCl_2$ and resuspended in 0.5% *n*-octyl-β,D-thioglucoside (OTG), 10 mM HEPES pH 7.0. Poly(butadiene)$_{12}$-Poly(ethylene oxide)$_8$ (PB_{12}-PEO_8) with carboxylic acid terminated polyethylene oxide[7] solubilized in 10 wt % OTG was mixed with PSI using a polymer to protein ratio (PoPR) w/w of 0.5 to 1.0 and a final concentration of 1.0 mg/mL PSI. The detergent concentration of the reconstitution mixture (60 µL) was adjusted to 4% and dialyzed against 0.5% OTG buffer containing 10 mM MES pH 6.0, 6 g/L ammonium ferric citrate, 3mM NaN_3 using 60 µL dialysis buttons (Hampton Research, Aliso Viejo, CA) for 24 hours at 25 ºC. The buttons were then transferred to detergent free buffer and dialyzed over a 72 hour period.

Electron Microscopy: PSI and detergent free membranes were adsorbed on glow-discharged carbon coated electron microscopy grids, stained with 0.75% uranyl formate, and imaged using a FEI Technai G2 Spirit BioTwin transmission electron microscope operating at 80 kV and equipped with an FEI Eagle 4k HS CCD.

Pump-Probe Optical Spectroscopy: Absorbance changes at 700 nm were measured using a commercial Joliot type pump-probe spectrophotometer, JTS-10 (Bio-Logic, France) at room temperature and at concentrations of 25 µg mL^{-1} Chl *a* (PSI in detergent micelles) and 50 µg mL^{-1} Chl *a* (PSI in BCP membranes). The buffer used contained 50 mM Tris-Cl pH 8.3, 10 mM NaCl, 10 mM $MgCl_2$, 10 µM 1,6-dichlorophenolindophenol (DCPIP), and 100 mM sodium ascorbate. Continuous actinic light was provided by the built-in orange LED array (940 µE m^{-2} s^{-1}). The probe beam was provided by the built-in white light LED source and a 700 nm interference filter (FWHM = 12 nm).

Preparation of electrodes: Glass slides coated with a 5 nm layer of chrome and a final 100 nm layer of gold (EMF corp., Ithaca, NY) were cleaned using a piranha solution (3:1 sulfuric acid and 30% hydrogen peroxide) (*caution*: Piranha solution is a strong oxidant and reacts violently with organic material) and washed with deionized water, then with ethanol and dried in a stream of nitrogen gas.

Cyclic voltammetry of bare gold electrode: Cyclic voltammetry was performed using a scan rate of 100 mV s^{-1} from -100 mV to 400 mV using Ag/AgCl reference electrode, Pt-wire counter electrode, and gold working electrode. The electrolyte solution contained 0.5 M KCl, 100 μM $K_3[Fe(CN)_6]^{3-}$, and 100 μM $K_4[Fe(CN)_6]^{4-}$.

Electrode Modification: A self-assembled monolayer was formed by applying to cleaned gold electrodes, 0.075 mM tethering PB_{12}-PEO_8 (T-PB), 0.075 PB_{12}-PEO_8, and 0.3 mM dithiodiglycolic acid for 1.0 hour. DSSN+ was then deposited onto the electrode in the presence of PB_{12}-PEO_8 and OTG (see SI for detailed protocol, figure and photograph).

Conjugated Oligoelectrolyte Synthesis: DSSN+ was synthesized as described previously. Briefly, an end-capped π-system was first prepared via a McMurry coupling (85% yield) of p-tolualdehyde followed by Wohl-Ziegler radical bromination (29% yield). The desired end-capped π-system with bisphosphonate was then generated by an Arbuzov reaction (55% yield). A subsequent Horner-Wadsworth-Emmons reaction and quaternization using trimethylamine afford the neutral chromophore DSSN (76% yield) and DSSN+ (73% yield). Both neutral and final products as well as the intermediates were characterized by ^{1}H and ^{13}C NMR spectroscopy, mass spectrometry, and elemental analysis.

Photocurrent Measurements: Block copolymer-photosystem I membranes were self-assembled at a PoPR 0.5-0.8 in 10 mM HEPES pH 7.0, 100 mM NaCl, 10mM $MgCl_2$, 3 mM NaN_3 for use

in photocurrent experiments. The reconstitution PSI membranes (0.09 mg PSI) were deposited onto the DSSN+/PB-PEO bilayer modified electrodes (2.8 cm^2). Photoelectrochemical measurements were completed on DSSN+/PB-PEO modified gold working electrodes with a BASi potentiostat (West Lafayette, IN) at room temperature using a working electrode bias of -300 mV, a Ag/AgCl reference electrode, and a Pt-wire counter electrode. Electrolyte solution contained 10 mM MES 6.0, 2 mM 1,1'-dimethyl-4,4'-bipyridinium (methyl viologen, Sigma-Aldrich), 100 μM PMS, 100 μM $K_3[Fe(CN)_6]^{3-}$, 100 μM $K_4[Fe(CN)_6]^{4-}$. Electrodes were illuminated with 1000 μmol m^{-2} s^{-1} (400 – 700 nm) (approximately 20 mW cm^{-2}) of light from an Oriel tungsten lamp.

Cryogenic transmission electron microscopy (Cryo-TEM): Samples were deposited on a holey carbon grid, plunged into liquid ethane and transferred in a cryogenic holder into a FEI Techai G2 Spirit BioTwin transmission electron microscope operating at 120 kV and equipped with an FEI Eagle 4k HS CCD.

77 K Fluorescence: Fluorescence excitation and emission spectra were measured with a SLM Model 8000C spectrofluorometer. Glycerol was added to a final concentration of 60 % to purified PSI.

UV-VIS: UV-Vis spectra were measured using NanoDrop 2000C spectrophotometer and were observed between wavelengths of 400 nm to 750 nm.

Fluorescence signal of DSSN+ on gold electrode: DSSN+ coated gold electrodes were fabricated as described in the methods section with the modification of using 2 mol % DSSN+ relative to PB_{12}-PEO_8 rather than 25 mol % to prevent poor imaging due to photobleaching. The electrodes were prepared for imaging by completely immersing them in deionized water, scratching a thin line of bilayer material off of the electrode surface with tweezers and the

covering the electrode with a glass coverslip (No. 1.5 Thermo Fisher) while submerged. The glass coverslip was cleaned with 7X detergent (MP-Biomedicals) prior to use. A thin layer of water was trapped between the glass coverslip and DSSN+ coated electrode, which preserved the structure of the bilayer. The electrodes were imaged with a Nikon Eclipse Ti-U inverted microscope equipped with a Lumencor Sola SMII light source and Andor iKon-M camera. A Nikon Plain Apo 20X objective was used for imaging. The DSSN+ coated electrode was imaged using an excitation wavelength of 488 nm and emission wavelengths above 520 nm. Images were analyzed using the image analysis program Metamorph.

Fluorescence Recovery After Photobleaching (FRAP*):* The mobility of DSSN+ in polymer-coated electrodes was measured using Fluorescence Recovery After Photobleaching. The samples were prepared as described in the preceding Fluorescence Imaging section. FRAP experiments were conducted using a Nikon TE2000-U inverted microscope equipped with a 10x objective, an X-Cite Series 120 Q light source and a Micromax 1024b CCD camera (Princeton Instrmuents). DSSN+ was bleached with a 473 nm diode laser with a power of 20 mW (Changchun New Indsutries Optoelectronics Technology Co., Ltd., Changchun, China). The diameter of the laser spot at the sample was approximately 30 micrometers. The sample was imaged before bleaching and after bleaching at 30 second time intervals. The fluorescence recovery was calculated as a function of time by measuring the average fluorescence intensity of DSSN+ in the bleached spot. The fluorescence intensity in the spot (red circle in Fig. S8,A-C) was normalized to the fluorescence of an unbleached section of the polymer-coated electrode (yellow circle in Fig. S8,A-C) in order to correct for photobleaching during imaging. The % recovery was found using Equation 8, where F_0 is the normalized fluorescence intensity of the spot immediately after bleaching and F_t is the intensity of the bleached spot at time t. The FRAP

curves from three separate experiments is plotted in Fig. S8,D. Due to the low fluorescence intensity of DSSN+, these measurements are within experimental error and suggest that DSSN+ is immobile in the polymer layer.

$$\frac{F_t - F_0}{1 - F_0} = \%\,\text{Recovery} \qquad \text{(Equation 1)}$$

UV polymerization of DSSN+/BCP interface: The interface was prepared above in "Electrode Modification," with the addition of 10% azobisisobutyronitrile (AIBN). The modified electrodes were exposed to 12 hours of UV light.

Stability of DSSN+/BCP and PSI electrodes: The photocurrent of the DSSN+/COE bilayer was measured weekly on modified gold working electrodes with a BASi potentiostat at room temperature using a working electrode bias of -300 mgV, a Ag/AgCl reference electrode, and a Pt-wire counter electrode. The electrodes were stored in dark conditions at 4 ºC between measurements. Electrolyte solution was remade daily and contained 10 mM MES 6.0, 2 mM 1,1'-dimethyl-4,4'-bipyridinium (methyl viologen, Sigma-Aldrich), 100 μM PMS, 100 μM $K_3[Fe(CN)_6]^{3-}$, 100 μM $K_4[Fe(CN)_6]^{4-}$. Electrodes were illuminated with 1000 μmol m^{-2} s^{-1} (400 – 700 nm) (approximately 20 mW cm^{-2}) of light from an Oriel tungsten lamp

References

1. R. De Zorzi, W. V. Nicholson, J.-M. Guigner, F. Erne-Brand and C. Vénien-Bryan, *Biophysical journal*, 2013, **105**, 398-408.
2. M. D. McConnell, R. Koop, S. Vasil'ev and D. Bruce, *Plant physiology*, 2002, **130**, 1201-1212.
3. M. Deverall, E. Gindl, E.-K. Sinner, H. Besir, J. Ruehe, M. J. Saxton and C. Naumann, *Biophysical journal*, 2005, **88**, 1875-1886.
4. G. Srinivas, D. E. Discher and M. L. Klein, *Nature materials*, 2004, **3**, 638-644.
5. J. Hinks, Y. Wang, W. H. Poh, B. C. Donose, A. W. Thomas, S. Wuertz, S. C. J. Loo, G. C. Bazan, S. Kjelleberg and Y. Mu, *Langmuir*, 2014, **30**, 2429-2440.
6. M. A. Hillmyer and F. S. Bates, *Macromolecules*, 1996, **29**, 6994-7002.

7. R. Nehring, C. G. Palivan, O. Casse, P. Tanner, J. Tüxen and W. Meier, *Langmuir*, 2008, **25**, 1122-1130.
8. S. Belegrinou, J. Dorn, M. Kreiter, K. Kita-Tokarczyk, E.-K. Sinner and W. Meier, *Soft Matter*, 2010, **6**, 179-186.
9. N. L. Mora, J. S. Hansen, Y. Gao, A. A. Ronald, R. Kieltyka, N. Malmstadt and A. Kros, *Chemical Communications*, 2014, **50**, 1953-1955.
10. J. Cras, C. Rowe-Taitt, D. Nivens and F. Ligler, *Biosensors and Bioelectronics*, 1999, **14**, 683-688.
11. N. Li, P. V. Warren, J. H. Golbeck, G. Frank, H. Zuber and D. A. Bryant, *Biochimica et Biophysica Acta (BBA)-Bioenergetics*, 1991, **1059**, 215-225.
12. R. C. Ford, A. Hefti and A. Engel, *EMBO J*, 1990, **9**, 3067.